Early-Time Dynamics and Reactivity of Polyoxometalate Excited States. Identification of a Short-Lived LMCT Excited State and a Reactive Long-Lived Charge-Transfer Intermediate following Picosecond Flash Excitation of $[W_{10}O_{32}]^{4-}$ in Acetonitrile

Dean C. Duncan,[†] Thomas L. Netzel,*[,‡] and Craig L. Hill*[,†]

Departments of Chemistry, Emory University, Atlanta, Georgia 30322, and Georgia State University, Atlanta, Georgia 30303

Received January 10, 1995[⊗]

We report here picosecond flash excitation results on $[W_{10}O_{32}]^{4-}$, **1**, which demonstrate that the initially prepared ligand-to-metal charge-transfer (LMCT) excited state decays within ~30 ps to a single intermediate, **2**, that persists for >15 ns. Little or no substrate reaction is derived from the short-lived LMCT excited state. Furthermore, the long-lived intermediate, **2**, *is not* the 1-electron-reduced species $[W_{10}O_{32}]^{5-}$, **3**, or one of its protonated derivatives. This long-lived intermediate, **2**, is the primary photoreactant and has substantial charge-transfer character itself. Additionally, **2** and **3** are likely to have similar W-orbital electron density; the principal differences in electronic structure derive from the presence of an oxidized oxygen site in **2** which is lacking in **3**.

Introduction

High-valent early-transition-metal oxygen anion clusters, known collectively as polyoxometalates, form a large and structurally diverse class of inorganic compounds with significant applications in several areas.[1-4] The rich and diverse genre of transformations involving substrates from alkanes to complex materials photosensitized by these complexes remains an area of active research.[4] However, only a few investigations address the primary photoevent and several points remain unclear.[5-10] In particular, further work is necessary to clarify the nature of the reactive polyoxometalate intermediate and the relevant time scale for substrate reaction. This is especially true for polyoxotungstates.

Previous studies on two *polyoxotungstates*, $[W_{10}O_{32}]^{4-}$ (nanosecond transient absorbance)[7] and $[PW_{12}O_{40}]^{3-}$ (fluorescence lifetime quenching),[8] suggest in both cases that the reactive intermediate is a rapidly relaxing (subnanosecond) electronically excited state which undergoes diffusion-controlled reactive quenching by a substrate either present in high concentration or complexed to the polyanion prior to excitation.[7,8] Other indirect evidence in support of this view derives from product yield and kinetics measurements obtained under both steady-state illumination and competitive substrate conditions.[11,12]

In the case of *polyoxomolybdates*, and for $[Mo_7O_{24}]^{6-}$ in particular, the situation appears to be different.[9,10] From picosecond transient absorbance measurements on $[Mo_7O_{24}]^{6-}$, Ferraudi *et al.*[9] propose an *unobserved* rapid decay of the $[Mo_7O_{24}]^{6-}$ excited state to a reactive intermediate with a lifetime (τ) of 33 ns. They state that this long-lived transient cannot be identified as an excited state. We presume this conclusion derives from both its long life and lack of emission.[13] Furthermore, the expected products (reduced $[Mo_7O_{24}]^{(6+x)-}$) are unstable and have not been independently synthesized.[14] In contrast, the large number of well-characterized reduced polyoxometalate complexes (known as heteropolyblues)[15-19] does permit their identification by picosecond transient absorbance spectroscopy after photoexcitation of their precursors. We chose to study the polyoxotungstate $[W_{10}O_{32}]^{4-}$, **1**, for three reasons: (1) Its reduced complexes are well characterized.[20-22] (2) A previous nanosecond transient absorbance study of it has already been published.[7] (3) **1** is among the most photochemically active polyoxometalates which promote alkane oxida-

[†] Emory University.
[‡] Georgia State Univeristy.
[⊗] Abstract published in *Advance ACS Abstracts,* August 1, 1995.

(1) Pope, M. T.; Müller, A. *Angew. Chem., Int. Ed. Engl.* **1991**, *30*, 34–48.
(2) *Polyoxometalates: From Platonic Solids to Anti-retroviral Activity*; Pope, M. T., Müller, A., Eds.; Kluwer Academic Publishers: Dordrecht, The Netherlands, 1993.
(3) Papaconstantinou, E. *Chem. Soc. Rev.* **1989**, *18*, 1–31.
(4) Hill, C. L.; Prosser-McCartha, C. M. In *Photosensitization and Photocatalysis Using Inorganic and Organometallic Complexes*; Kalyanasundaram, K., Grätzel, M., Eds.; Kluwar Academic Publishers: Dordrecht, The Netherlands, 1993; Chapter 13, pp 307–330.
(5) Polyoxometalate electron-donor acceptor complexes exhibit transient behavior different from that of the systems addressed here.[6]
(6) (a) Schmidt, J. A.; Hilinski, E. F.; Bouchard, D. A.; Hill, C. L. *Chem. Phys. Lett.* **1987**, *138*, 346. (b) Hill, C. L.; Bouchard, D. A.; Kadkhodayan, M.; Williamson, M. M.; Schmidt, J. A.; Hilinski, E. F. *J. Am. Chem. Soc.* **1988**, *110*, 5471.
(7) Yamase, T.; Usami, T. *J. Chem. Soc., Dalton Trans.* **1988**, 183.
(8) Fox, M. A.; Cardona, R.; Gaillard, E. *J. Am. Chem. Soc.* **1987**, *109*, 6347.
(9) Kraut, B.; Ferraudi, G. *Inorg. Chem.* **1989**, *28*, 2692.
(10) (a) Kraut, B.; Ferraudi, G. *Inorg. Chem.* **1990**, *29*, 4834. (b) Kraut, B.; Ferruadi, G. *J. Chem. Soc., Dalton Trans.* **1991**, 2063.
(11) Hill, C. L.; Renneke, R. F.; Combs, L. *Tetrahedron*, **1988**, *44*, 7499.
(12) Hill, C. L.; Renneke, R. F.; Combs, L. A. *New J. Chem.* **1989**, *13*, 701.
(13) Over the first 100 ps there is a positive absorbance at 400 nm which later bleaches at times >3 ns. The connection between these two signals is puzzling.
(14) Photoexcitation leads to permanent spectral changes assigned to reduced Keggin-type polyoxomolybdate. See: Yamase, T.; Sasaki, R.; Ikawa, T. *J. Chem. Soc., Dalton Trans.* **1981**, 628.
(15) Pope, M. T. *Heteropoly and Isopoly Oxometalates*; Springer Verlag: New York, 1983; Chapter 6.
(16) (a) Sanchez, C.; Livage, J.; Launay, J. P.; Fournier, M.; Jeannin, Y. *J. Am. Chem. Soc.* **1982**, *104*, 3194. (b) Sanchez, C.; Livage, J.; Launay, J. P.; Fournier, M. *J. Am. Chem. Soc.* **1983**, *105*, 6817.
(17) Barrows, J. N.; Pope, M. T. *Inorg. Chim. Acta* **1993**, *213*, 91 and references cited therein.
(18) Casañ-Pastor, N.; Baker, L. C. W. *J. Am. Chem. Soc.* **1992**, *114*, 10384–10394 and references cited therein.
(19) Fruchart, J. M.; Hervé, G.; Launay, J. P.; Massart, R. *J. Inorg. Nucl. Chem.* **1976**, *38*, 1627.
(20) Chemseddine, A.; Sanchez, C.; Livage, J.; Launay, J. P.; Fournier, M. *Inorg. Chem.* **1984**, *23*, 2609.
(21) Duncan, D. C.; Hill, C. L. Manuscript in preparation.
(22) Yamase, T. *J. Chem. Soc., Dalton Trans.* **1987**, 1597.

0020-1669/95/1334-4640$09.00/0 © 1995 American Chemical Society

tion.[7,11,12,23-28] We report here picosecond flash excitation results on **1** which demonstrate that the initially prepared ligand-to-metal charge-transfer (LMCT) excited state decays within ~30 ps to a single intermediate, **2**, that persists for >15 ns. Little or no substrate reaction is derived from the short-lived LMCT excited state. Furthermore, the long-lived intermediate, **2**, *is not* the 1-electron-reduced species $[W_{10}O_{32}]^{5-}$, **3**, or one of its protonated derivatives. This long-lived intermediate is the primary photoreactant and has substantial charge-transfer character itself. Additionally, **2** and **3** are likely to have similar W-orbital electron density; the principal differences in electronic structure derive from the presence of an oxidized oxygen site in **2** which is lacking in **3**.

Experimental Section

Transient Absorbance Measurements. The actively and passively mode-locked Nd:YAG laser (λ = 1064 nm; 15 Hz repetition rate; ~30 ps fwhm) system was manufactured by Quantel International, Inc. The pulse generation portion of this system consisted of an oscillator (4-mm-diameter rod), an extra-cavity Pockels cell with crossed polarizers, and a preamplifier (7-mm-diameter rod, single pass) whose output was spatially filtered and recollimated. At this point each pulse was split into four beams. Three of these beams (A_1, A_2, and A_3 in Figure 1) each were directed through a single-pass amplifier (7-mm-diameter rod), and one (A_4) was directed through a double-pass amplifier (9-mm-diameter rod). The amplifier rods were underfilled with no circular diffraction effects visible on burn paper. Vacuum spatial filtering of the double-pass output was an option which was not used in the experiments described here. Pulse energies of up to 35 and 70 mJ, respectively, were achieved easily with the single- and double-pass amplifiers. The Pockels cell (SPS411) originally supplied by Quantel employed avalanche transistors. However, the stability of the laser's output was improved (2- to 3-fold) by replacing this unit with one based on a microwave triode (Medox Electrooptics, DR87-UFD).

A schematic diagram of the rest of the picosecond transient absorbance spectrometer is presented in Figure 1. This arrangement is built upon one described earlier.[29] To minimize losses, all optical surfaces are coated with high-power dielectric films. Importantly, transmission optics have antireflection (AR) coatings for specified wavelengths; reflection optics are coated for maximum reflection at specified wavelengths, polarizations, and angles of incidence. Optical paths, A_3 and A_4, are used in the transient absorbance experiment as the pump and probe beams, respectively. This arrangement allows for an adjustable excitation energy without compromising the stability of the continuum probe beam. The other two paths, A_1 and A_2, are directed to other laser tables and are used in other experiments such as emission lifetime measurements. In each path, the first half-wave (λ/2) plate allows the linear polarization to be adjusted as needed for the generation of harmonics. The final angle-tuned harmonic generating crystals (KD*P) in each path are set to produce a horizontally polarized output (A_3 = 355 nm; A_4 = 532 nm). The fundamental and harmonic wavelengths in each beam are then separated with a Pellin-Broca prism (Brewster angle input), and the undesired wavelengths are blocked with an iris.

An 8-ft optical delay line consisting of a GPIB-controlled translation stage (Anorad-10 System, Anorad Corp.) and a glass AR-coated retroreflector provides up to 16 ns of total delay in the A_4 path with a precision of ±0.03 ps. Continuum probe light is generated by focusing the A_4 beam (λ = 532 nm) with a lens (800 mm f.l., *f*/32) to a point located about two-thirds of the way inside a 20-cm cell containing 0.5-μm filtered D_2O/H_2O (80:20, v/v). Stable generation of the continuum probe beam requires ~10 mJ/pulse; importantly, no damage of optical components occurs at this energy. Additionally, the probe beam's stability is optimized by tuning the oscillator's pump voltage and monitoring the probe light (*vide infra*). This probe light is collected with a visible achromatic lens (147 mm f.l., *f*/3); the residual λ = 532 nm laser light is rejected with suitable cut off or interference filters; and the desired probe light is focused onto a 0.8-mm-diameter aperture in contact with a lightly sand-blasted quartz slide. This diffuser slide serves three purposes: it spatially homogenizes the probe light; it partially depolarizes the light; and it provides a point source for subsequent imaging. Furthermore, this arrangement decouples the alignment of optics located before and after the diffuser as described previously.[29] Additionally, a quartz achromatic depolarizer placed immediately after the diffuser further enhances probe light depolarization. Next, the diffuser's light is collected and crisply imaged (1:1) with a visible achromat (36-cm f.l., *f*/15) at the center of the sample cell. This lens is the limiting aperture in the probe beam's optical train. A broad-band cube beamsplitter (Melles Griot, 03 BSC015) is placed midway between this visible achromat and the sample cell. The reflected portion is used for the reference beam. Sample and reference beams are each imaged with separate achromatic lenses onto the entrance slits of separate 0.25-m double monochromators (Model DH10, Instruments SA, Inc.; 1-mm slits, 2 mm/nm dispersion, 500-nm grating blaze). These imaging lenses are underfilled, and each is positioned respectively 40 cm from its probe beam image and 10 cm from its monochromator slit such that the probe light perfectly fills each monochromator's gratings (*f*/3.5) with no losses at their edges. The light is detected with five-stage red-enhanced alkali photomultiplier tubes (PMT, Hamamatsu R928).

The excitation beam energy is monitored by observing a small fraction of the beam which "leaks" through a reflector onto a PMT. Prior to sample excitation, the beam is circularly polarized to eliminate polarization artifacts due to photoselective excitation. The beam is condensed to a 3-mm diameter with an inverted Galilean telescope and enters the sample cell at a narrow angle (~2°) relative to the cell face normal. The probe beam volume is well contained within the excitation beam volume throughout the 1-cm cell path.

To eliminate laser system RF interference within the excitation and probe beam electronics, an optical trigger signal is produced by focusing a stray reflection of the A_4 532-nm beam into a 25-ft optical fiber. Additionally, all detection electronics (sample/hold and ADC circuits) are powered by a separate isolation transformer. The fiber's output light is detected by a photodiode in a triggering/timing sequencer designed and built by Lee Rogers, Brookhaven National Laboratory, Instrumentation Division (IO-445) which generates a master trigger for sample/hold and ADC modules. The photoinduced charges derived from detection of the excitation, sample, and reference beams are each preamplified and pulse-shaped at the PMT. These shaped pulses are sent to separate sample/hold NIM modules from which their peak heights are passed to Lecroy Model 3511 12-bit ADCs. Tests confirm that the digitized voltages are linearly proportional to the photoinduced charges on the PMT anodes. The digitized voltages are then transmitted to a PC486 computer using a Lecroy 4802 CabG GPIB CAMAC Crate Controller and a Lecroy 8901A GPIB interface. The wavelength settings of the sample and reference monochromators are selected by stepping motors which are driven by CAMAC-mounted stepping motor controllers (Kinetic Systems Model 3362). Uniblitz electromechanical shutters are placed in the A_3 and A_4 beam paths after the Pellin-Broca prism/iris pair. These shutters control the transmission of pump and probe beams and are operated by a CAMAC IGOR module (Kinetic Systems Model 3063). Custom FORTRAN programs (Dennis Williamson, Amoco Technology Corp., Naperville, IL) control data acquisition, operation of the optical delay stage, shutter motion, and monochromator setting.

The electromechanical shutters permit data accumulation with and without sample excitation. Each primitive absorbance change (ΔA) data point is obtained at a given time (delay stage setting) and

(23) (a) Renneke, R. F.; Hill, C. L. *Angew. Chem. Int. Ed. Engl.* **1988**, *27*, 1526. (b) Renneke, R. F.; Pasquali, M.; Hill, C. L. *J. Am. Chem. Soc.* **1990**, *112*, 6585. (c) Renneke, R. F.; Kadkhodayan, M.; Pasquali, M.; Hill, C. L. *J. Am. Chem. Soc.* **1991**, *113*, 8357. (d) Combs-Walker, L. A.; Hill, C. L. *J. Am. Chem. Soc.* **1992**, *114*, 938.
(24) Hill, C. L.; Kozik, M.; Winkler, J.; Hou, Y.; Prosser-McCartha, C. M. *Adv. Chem. Ser.* **1993**, *238*, 243–259.
(25) Renneke, R. F. Ph.D. Dissertation, Emory University, 1989.
(26) Maldotti, A.; Amadelli, R.; Varani, G.; Tollari, S.; Porta, F. *Inorg. Chem.* **1994**, *13*, 2968.
(27) Attanasio, D.; Bachechi, F. *Adv. Mat.* **1994**, *6*, 145.
(28) Moriguchi, I.; Hanai, K.; Hoshikuma, A.; Teraoka, Y.; Kagawa, S. *Chem. Lett.* **1994**, *4*, 691.
(29) Winkler, J. R.; Netzel, T. L.; Creutz, C.; Sutin, N. *J. Am. Chem. Soc.* **1987**, *109*, 2381.

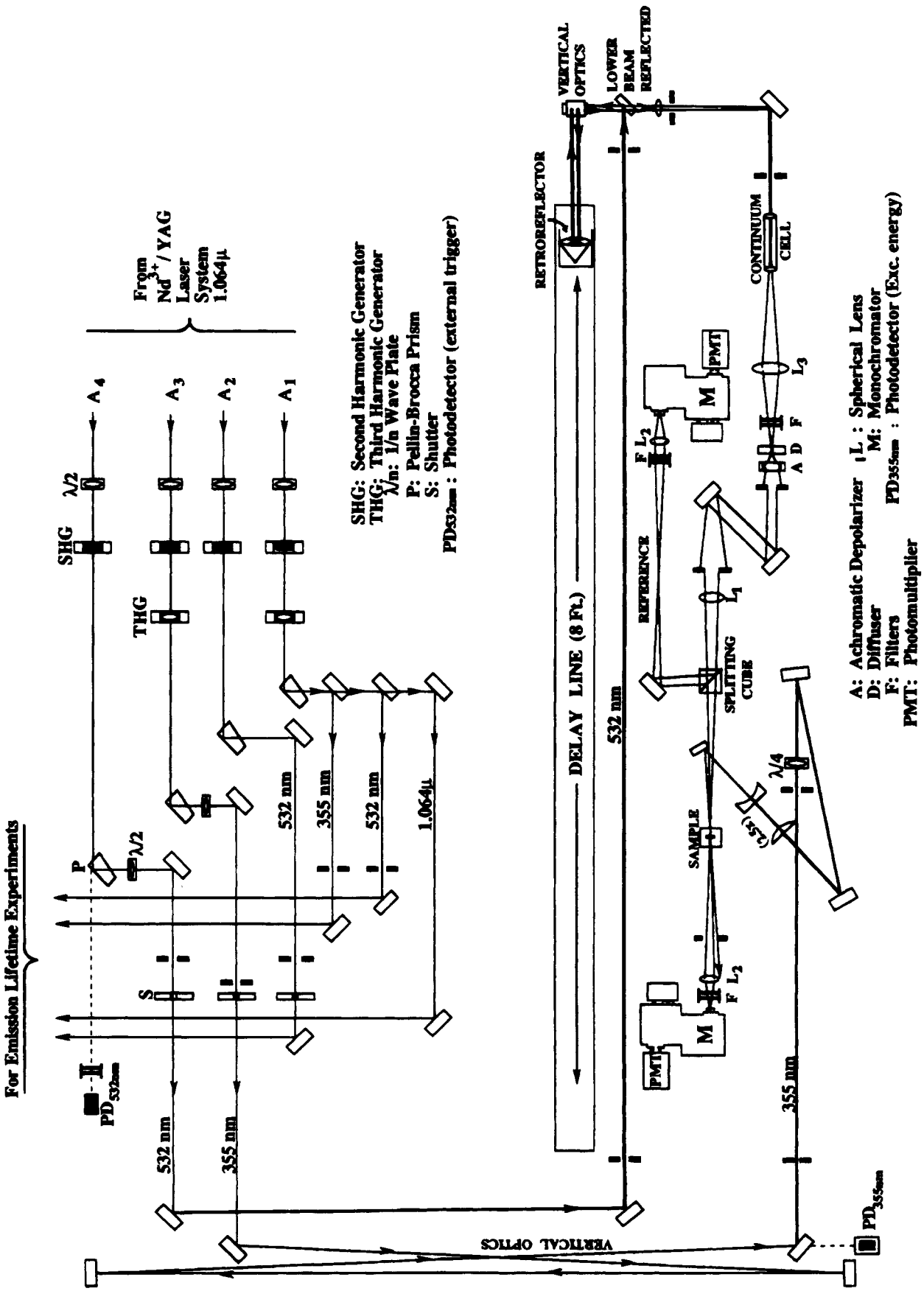

Figure 1. Schematic drawing of the picosecond transient absorbance spectrometer.

wavelength and consists of a two-cycle sequence of 240 laser-firings (shots): one cycle is composed of 60 shots with excitation and 60 shots without excitation. For each laser shot, the sample and reference signals are ratioed. After the first cycle, ΔA values are calculated from the ratio averages obtained with and without excitation (60 shots each). Then this cycle is repeated, and the resulting two ΔA values are averaged to provide a single primitive ΔA data point (240 shots). This two-cycle sequence reduces systematic error by interleaving sets of 60-shot cycles with and without excitation. However, to maximize signal-to-noise in the experiments reported here, eight primitive ΔA data points were accumulated and averaged for each ΔA data point plotted. Thus, here each plotted ΔA point reflects data from 1920 laser shots. The ΔA errors in the plots are plus-or-minus one standard deviation.

In the collection of a primitive ΔA data point, sample and reference beam ratios are averaged only if the ADC values of the excitation, sample and reference beams fall inside specified upper and lower ranges. This ensures uniform excitation conditions throughout kinetics or spectral measurements. For obtaining kinetics or difference spectra, ΔA points (1920 averaged shots each) are interleaved randomly in either time or wavelength. Zero-time positions in kinetics plots are arbitrary reference points. In the visible region, this instrument yields ΔA errors of ± 0.001; larger errors occur in the near-UV and near-IR regions.

A positive displacement gear-pump (Cole-Parmer Micropump H-07002-23) with a magnetically coupled stainless steel head and Teflon-clad gears circulates the sample solution in a closed system. Teflon tubing connects the following three components with the pump head: a 100-mL round-bottom flask sample reservoir equipped with a rubber septum and two 16-gauge SS inlet/outlet needles; a filter (Millipore, 0.5 μm) at the reservoir inlet; and a 1-cm quartz optical flow cell. This cell is masked to prevent scattered light from reaching the detector. All glass−Teflon and metal−Teflon tubing junctions are hermetically sealed with heat-shrink Teflon tubing and epoxy resin. Boil-off N_2 gas is available for deaeration by bubbling. The solution flow is increased while ΔA spectral changes are monitored at a transient absorbance maximum (or minimum) until ΔA changes at −500 ps delay are zero.

Transient yields derived from excitation of acetonitrile solutions containing **1** ($(1-5) \times 10^{-4}$ M; ~50 mL) were not dependent on the presence of ambient atmospheric oxygen up to 15 ns after photoexcitation. Consequently, the experiments reported here were performed without deaeration. Additionally, the presence of O_2 minimized the buildup of reduced decatungstate photoproducts. Absorbance spectra (UV−vis) were recorded before and after data collection. Net spectral changes were not observed in any of the samples after kinetics study. Additionally, during the acquisition of kinetics or spectral data, a characteristic transient ΔA (λ_{max} = 780 nm; 0.5 ns delay) was monitored before, during, and after the experiment as a check for systematic errors. Finally, acetonitrile solutions of **1** were tested for linear variation of ΔA signals with excitation energy (Figure 2). All data reported here were obtained at excitation energies well below those that induced saturation.

Materials and Synthesis. Acetonitrile and 2-butanol were purchased from B&J and used as received. Tetra-*n*-butylammonium bromide (QBr), QPF_6, and $Na_2WO_4{\cdot}2H_2O$ were purchased from Aldrich, Bioanalytical Systems, and Johnson-Matthey, respectively. High-purity cyclohexene (99+%) was obtained from Fluka.

The tetra-*n*-butylammonium (Q) salt of **1**, $Q_4[W_{10}O_{32}]$ (Q**1**), and the corresponding Na^+ salt (Na**1**) were prepared according to modified published procedures and characterized by ^{183}W NMR, UV−vis, and IR spectroscopy.[20,25]

$Q_4[W_{10}O_{32}]$. Boiling 3 M HCl (134 mL) was added to a boiling solution of $Na_2WO_4{\cdot}2H_2O$ (64 g) in distilled water (400 mL), and the mixture was allowed to stir for 1 min. An aqueous solution (40 mL) containing QBr (25.6 g) was added with rapid stirring and the resulting mixture allowed to cool to ambient temperature. The precipitate was collected on a frit, washed with hot water, ethanol, and diethyl ether, and air-dried. The complex, **1**, was very soluble in acetonitrile (>0.15 M). This precipitate was taken up in a minimum of hot acetonitrile, and the mixture was filtered to remove a white slightly soluble residue

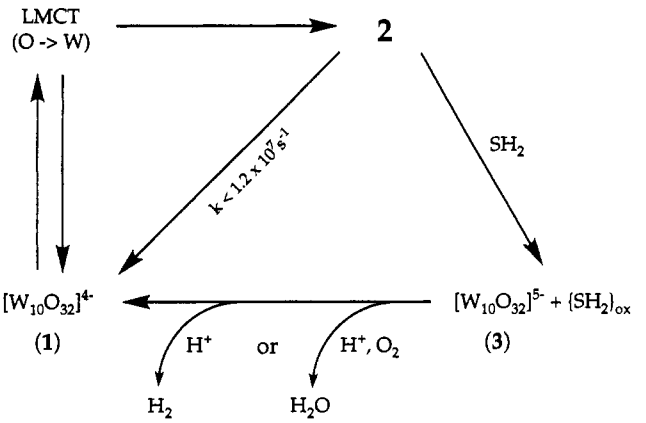

Figure 2. Scheme for the excited-state transformations of $[W_{10}O_{32}]^{4-}$, **1**. The initially photoexcited LMCT state ($\tau \leq 30$ ps) decays to form **2**, which oxidizes organic substrates, SH_2, producing **3** and oxidation products, $\{SH_2\}_{ox}$. Reoxidation of **3** (or other reduced species derived from **3**) can occur either by hydrogen evolution or by dioxygen reduction.

(probably ψ-metatungstate).[30,31] Crystals from the intensely green filtrate were obtained either by slow evaporation or by adding diethyl ether and storing at 0 °C. Contamination of the product with ψ-metatungstate was indicated by an increase in the relative absorbance ($A_{\lambda 268}/A_{\lambda 324}$) from 1.14.

$Na_4[W_{10}O_{32}]$. To a boiling solution containing $Na_2WO_4{\cdot}2H_2O$ (66 g) in distilled water (400 mL) was added 400 mL of a boiling aqueous 1 M HCl solution. The resulting solution was allowed to boil for 10 s, divided into two equal portions in 2-L beakers, and *rapidly* cooled to 30 °C in a dry ice/methanol bath with stirring. Solid NaCl was added to near saturation, and the mixture was cooled further to 0 °C. A precipitate formed, which was collected and dried on a fritted funnel (33 g). This precipitate was suspended in hot acetonitrile (200 mL), the suspension was filtered, and the filtrate was placed in a freezer overnight. Large pale-lime crystalline rectangular blocks of Na**1** were collected and dried on a fritted funnel (11.19 g).[32] The absorbance spectrum of both Q**1** and Na**1** in acetonitrile consisted of a well-defined maximum at 324 nm (ϵ = 14 100 M^{-1} cm^{-1}) assigned previously to an O → W LMCT transition.[33] This band tailed into the visible region and disappeared around 420 nm.

The reduced complex $[W_{10}O_{32}]^{5-}$, **3**, was prepared in acetonitrile within a glovebox by controlled-potential electrolysis at −1.47 V vs 0.01 M $Ag/AgNO_3$ on carbon cloth using a 100-fold molar excess QPF_6 as the electrolyte. Details of this synthesis will be published elsewhere.[21] The UV−vis spectral properties of **3** in acetonitrile were identical with those of **3** prepared in DMF: absorbance maxima at 370 nm (ϵ = 6700 M^{-1} cm^{-1}) and 780 nm (ϵ = 7000 M^{-1} cm^{-1}).[20,21]

Results and Discussion

A model for the photoinduced changes in **1** consistent with the picosecond transient absorption data is shown in Figure 2. Figure 3 shows a linear relationship between the excitation energy and the transient absorbances (2−14 mJ/cm^2) observed at 390, 690, and 780 nm. All kinetics and spectral data described here were collected well within this energy range. Additionally, other experiments (data not shown) demonstrated that the transient absorbance temporal behavior of both Q**1** and Na**1** in acetonitrile (λ_{exc} = 355 nm, ~30 ps (fwhm); 4−12 mJ/cm^2; $(1-5) \times 10^{-4}$ M) observed at ~50 nm intervals *in the range 440−800 nm* was invariant from the time of excitation to 15 ns after excitation. Figure 4 shows difference spectra recorded at 0.5 ns (top) and 14.5 ns (bottom), and Figure 5

(30) Souchay, P.; Boyer, M.; Chauveau, F. *Trans R. Inst. Technol. Stockholm* **1972**, *259*, 161.
(31) Le Meur, B.; Souchay, P.; Chauveau, F. *Rev. Chim. Miner.* **1973**, *10*, 711.
(32) For an alternative preparation see ref 25.
(33) Termes, S. C.; Pope, M. T. *Inorg. Chem.* **1978**, *2*, 500.

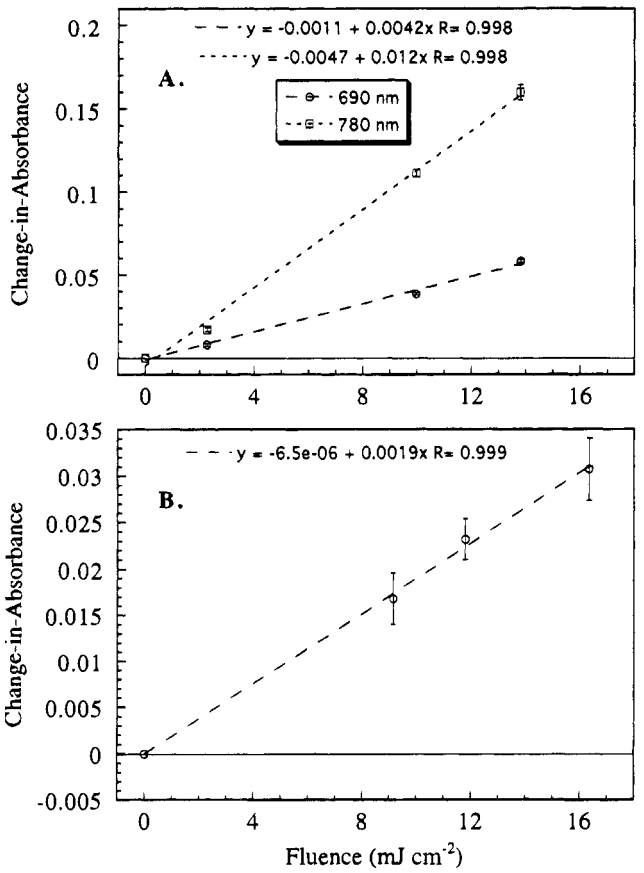

Figure 3. Dependence of transient absorbance (ΔA) on 355-nm excitation fluence for a 5×10^{-4} M $Q_4[W_{10}O_{32}]$ acetonitrile solution: (A) 690 nm (500 ps delay) and 780 nm (500 ps delay); (b) 390 nm (data taken during photoexcitation at the peak ΔA).

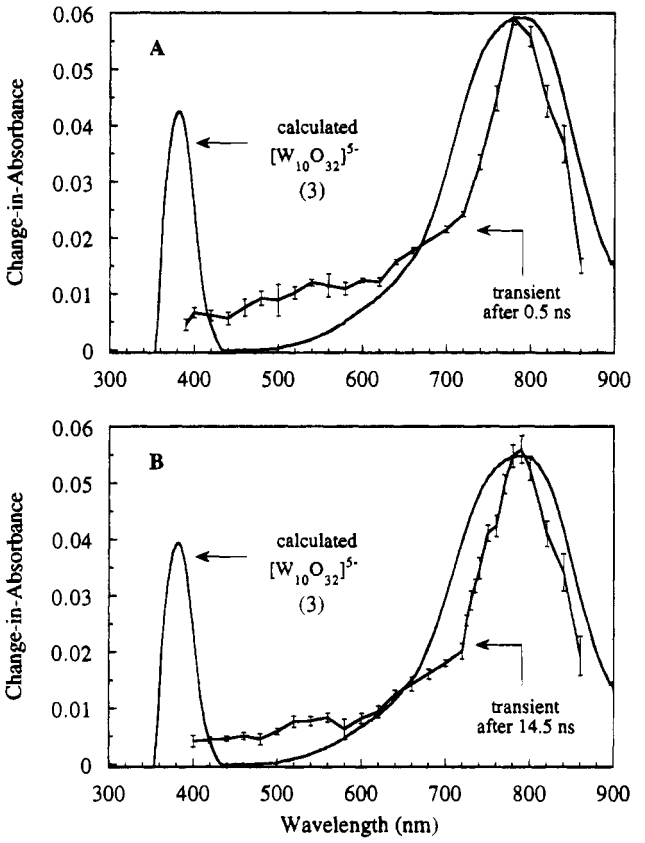

Figure 4. Transient absorbance (ΔA) spectra (solid curves with error bars) obtained following 355-nm excitation (~6 mJ/cm^2) of a 5×10^{-4} M **Q1** acetonitrile solution: (A) 0.5 ns delay; (B) 14.5 ns delay. Also shown is a calculated difference spectrum (solid curve without error bars) of **3** in acetonitrile obtained by subtracting the extinction coefficients of **3** from those of **1** and normalizing the resulting 780 nm maximum to that of **2**.

showsa representative kinetics profile at 780 nm. Over the 440−800 nm range, the transient rise is excitation-pulse-limited (≤30 ps) and decays slowly with $\tau \geq 80$ ns (single-exponential fit, assuming $\Delta A = 0$ at $t = \infty$). This behavior is consistent with the production of a single long-lived transient, **2**, during photoexcitation.

However, Figure 6 shows different transient behavior *at 390 nm during photoexcitation.* After the initial rise (the maximum ΔA at 390 nm is about one-sixth that at 780 nm), the transient decays rapidly (~30 ps) to about half that of the peak maximum. *Following decay of this prompt absorbance transient, the kinetics data at 390 nm are similar to those observed at all other wavelengths.* This behavior is consistent with assigning the prompt absorbance transient at 390 nm to an LMCT excited state which subsequently generates **2**. The only detectable emission for **1** in acetonitrile (298 K) in the 400−900 nm range is a weak broad band (Stokes shift of 16 900 cm^{-1}) centered at 615 nm which has a lifetime <30 ps.[24] The excitation-pulse-limited relaxations of both the emission and the 390-nm prompt absorbance transient suggest that both originate from the same LMCT state.

Two lines of evidence indicate that **2** is not the reduced complex $[W_{10}O_{32}]^{5-}$, **3**, or a protonated derivative of **3** as proposed previously.[7] The first line of evidence is that Figure 4 shows distinct differences between the transient absorbance spectrum of **2** and that calculated for **3**. The intermediate, **2** has a greater ΔA, from 400 to 560 nm, a narrower width for the 780-nm peak, and most significantly, a lack of ΔA increase in the 390−420 nm region relative to **3**. In previous work, the transient absorbance spectrum was recorded only over the 600−900 nm wavelength range.[7] Additionally, although no absorbance spectra exist for the $H_x[W_{10}O_{32}]^{(5-x)-}$ species (primarily due to rapid disproportionation), they are expected to be blue-shifted with respect to **3**.[16,19] The second line of evidence is that **Q1** transient absorbances (measured at times ≤1 ns as illustrated in Figure 6 at 390 nm) are not altered by the addition of reactive substrate. Additionally, Table 1 shows transient absorbances of **Q1** at 390 and 780 nm obtained in the presence and absence of two reactive substrates, 2-butanol (4 M; Φ = 0.39)[25,34] and cyclohexene (0.5 M; Φ = 0.06).[7,34,35] These ΔA measurements were made with constant excitation energy *in the ≤1-ns time region.* A related control experiment showed that both kinetics and transient absorbance measurements of **Q1** and **Na1** exhibited identical behavior at 780 nm, demonstrating a lack of counterion dependence (Q^+ is a potential substrate with Φ = 0.005−0.01).[34,36] These two lines of evidence demonstrate that **2** is neither the substrate-induced photoproduct, **3**, nor one of its protonated derivatives. Furthermore, these data collectively rule out the prior suggestion that substrate reaction sensitized by photoexcited **1** occurs predominantly within the flash due to precomplexation of substrate with **1** in its ground state; clearly little or no chemistry derives from the short-lived LMCT excited state.[5-7,11,12,24]

(34) The reported quantum yield is defined as 0.5 × (moles of electrons present in reduced complexes/einsteins of light absorbed).
(35) The authors in ref 7 claim transient absorbance detection of **3** at 780 nm within the 308 nm excitation pulse (10 mJ; ~10 ns fwhm). Their data indicate a substrate dependence (0.5 M cyclohexene) for the absorbance transient at 780 nm. This is not true for our observations (see Table 1).
(36) Yamase, T.; Takabayashi, N.; Kaji, M. *J. Chem. Soc., Dalton Trans.* **1984**, 793.

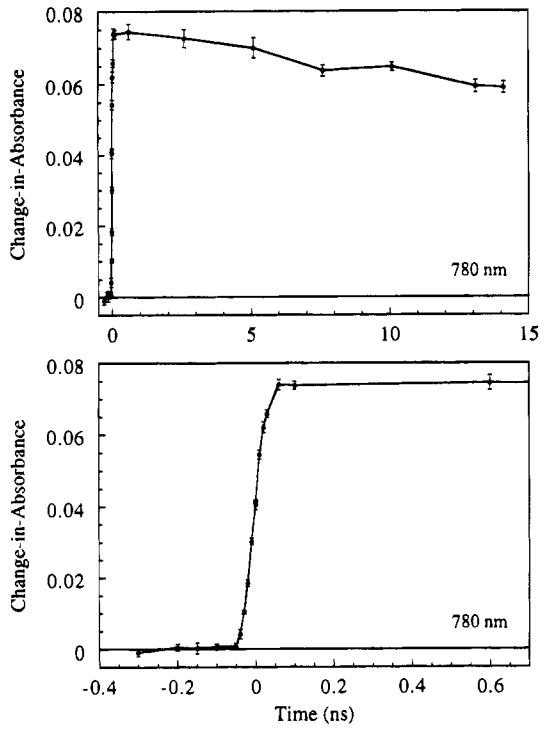

Figure 5. Representative kinetics observed at 780 nm for the absorbance transient produced following 355-nm excitation (~7 mJ/cm^2) of a 5 × 10^{-4} M **Q1** acetonitrile solution: (top) 0−15 ns delay; (bottom) −0.2 to +0.4 ns delay. Solid lines connect the data points for ease of visualization.

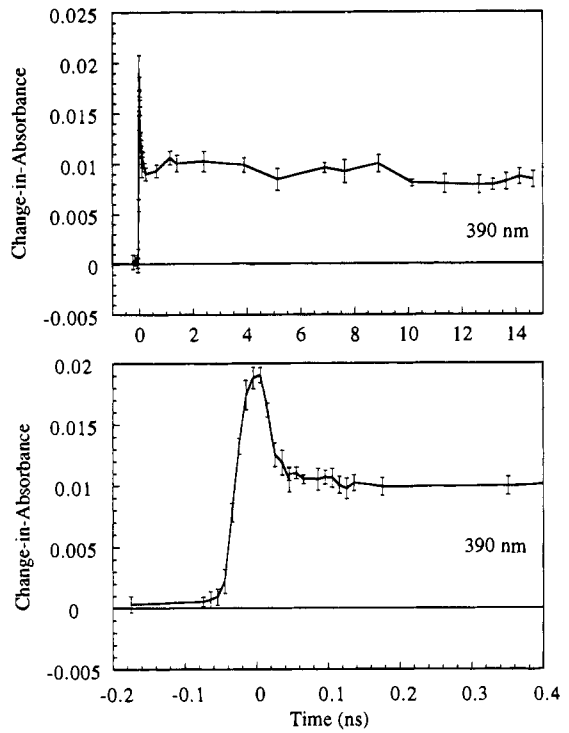

Figure 6. Early-time kinetics profile observed at 390 nm for the absorbance transient following 355-nm excitation (~10 mJ/cm^2) of a 5 × 10^{-4} M **Q1** acetonitrile solution: (top) 0−15 ns time range without added substrate; (bottom) −0.2 to +0.4 ns time range with 4 M 2-butanol added. Kinetics in the ≤1 ns time range do not depend on added reactive substrate. The excitation-pulse-limited rise of the initial transient is assigned to an LMCT excited state which decays within ~30 ps to form **2**. Solid lines connect the data points for ease of visualization.

Evidence that **2** is the reactive intermediate is shown in Figure 7. Transient absorbance detection of **3** with minimal interference from **2** is most clear at 390 nm (see Figure 4). In Figure 7, a small slowly rising absorbance increase at 390 nm is observed in the presence of either 4 M 2-butanol or 0.5 M cyclohexene *in the 1−15-ns time range*. This is consistent with biomolecular capture of a small fraction of **2** by substrate thereby generating the reduced complex **3**. Most of this substrate reaction occurs on a long time scale (probably >50 ns). Since the maximal rate constant for polyoxometalate diffusion-controlled reactions is ~10^{10} M^{-1} s^{-1}, so slow a reaction at high concentration of substrate implies that ~10^3−10^4 collisions are necessary for each reactive encounter. In addition, the similarity of the yields of **3** observed 15 ns after photoexcitation for 2-butanol and cyclohexene (see Figure 7) suggests that their different quantum yields (respectively 0.39 and 0.06)[7,25,35] may possibly derive from differing subsequent thermal reactions.

Comparison of the spectra of **2** and **3** (Figure 4) also suggests, however, that these two species may have some important

Table 1. Substrate Dependence of Q1 Transient Absorbance Yields[a]

substrate	ΔA_{780}[b]	$\Delta A_{390,peak}$[c]	$\Delta A_{390,baseline}$[d]
none	0.1145 ± 0.0040	0.0223 ± 0.0015	0.0109 ± 0.0015
4 M 2-butanol	0.1152 ± 0.0040	0.0200 ± 0.0020	0.0111 ± 0.0016
0.5 M cyclohexene	0.1110 ± 0.0035	0.0206 ± 0.0015	0.0109 ± 0.0013

[a] 355 nm picosecond flash excitation (~10 mJ/cm^2) of 5 × 10^{-4} M **Q1** acetonitrile solutions. All data were recorded under identical excitation conditions as described in the Experimental Section. [b] Points taken at 1 ns delay. [c] Points taken during photoexcitation at the peak ΔA. [d] Points taken after 100 ps delay.

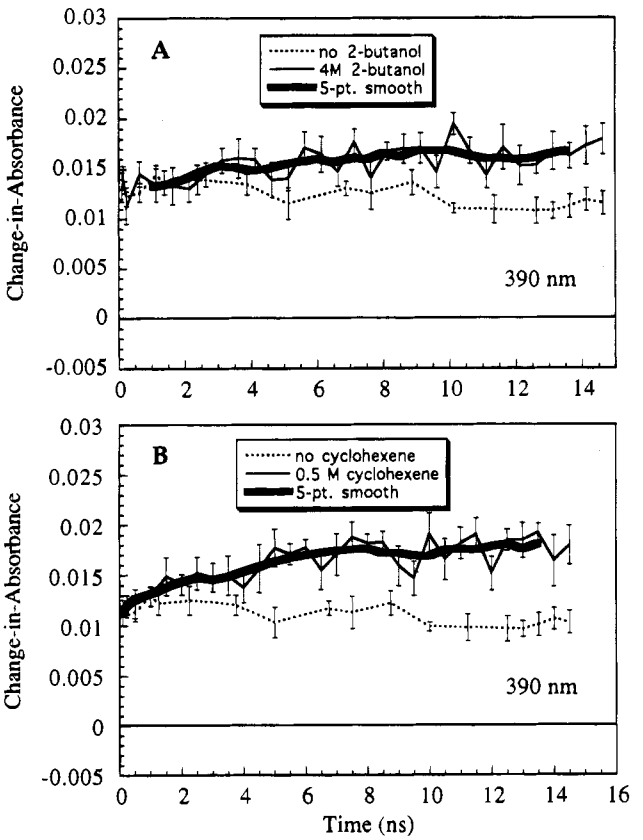

Figure 7. Kinetics profiles observed at 390 nm for the absorbance transients following 355-nm excitation (~11 mJ/cm^2) of 5 × 10^{-4} M **Q1** acetonitrile solutions with and without substrate: (A) 4 M 2-butanol substrate; (B) 0.5 M cyclohexene substrate. The broad lines in each plot are five-point moving averages through the data obtained in the presence of substrate. Bimolecular reactive capture of a small fraction of **2** by substrate is proposed to account for the slowly rising absorbance at 390 nm on this time scale.

electronic feature in common since they both absorb strongly at 780 nm. In reduced ground-state polyoxotungstates, the highest occupied molecular orbital (HOMO) is predominantly W-based.[1,15] In addition, the initially prepared LMCT state of **1** has two principal features: a highest energy valence electron also located in a predominantly W-based molecular orbital (MO) and a positively-charged hole located in a predominantly O-based MO.[20-22] Consequently, it is likely that important parts of both these features also are retained in **2**. The observed spectral differences between **2** and **3** in the 400-nm region (see Figures 4 and 7) may be due to the presence of an O-based hole in **2** and its absence in **3** due to reduction by substrate. Additional information will be needed to characterize further the electronic structure of **2** (*e.g.* time-resolved Raman or EXAFS spectroscopy). Transient absorbance investigations of **1** in the ns−ms time domain with a variety of substrates should provide needed information of the reactivity of **2**.

Acknowledgment. This work was supported by the U.S. Department of Energy, Office of Health and Environment, Radiological and Chemical Physics Research Division (Grant No. DE-FG05-03ER61604 to T.L.N.) and the National Science Foundation (Grant No. CHE-9412465 to C.L.H.).

IC950024K